Journal of the Korean Society for Nondestructive Testing
Vol. 30, No. 6 (2010. 12)

Effect of Hysteresis on Interface Waves in Contact Surfaces

Nohyu Kim*† and Seungyong Yang**

Abstract This paper describes a theoretical model and acoustic analysis of hysteresis of contacting surfaces subject to compression pressure. Contacting surfaces known to be nonlinear and hysteretic is considered as a simple spring that has a complex stiffness connecting discontinuous displacements between two solid contact boundaries. Mathematical formulation for 1-D interfacial wave propagation between two contacting solids is developed using the complex spring model to derive the dispersion relation between the interface wave speed and the complex interfacial stiffness. Existence of the interface wave propagating along the hysteretic interface is studied in theory and discussed by investigating the solution to the dispersion equation. Unlike the linear interface without hysteresis, there can exist only one distinct mode of interface waves for the hysteretic interface, which is anti-symmetric motion. The anti-symmetric mode of interface wave propagates with the velocity faster than the Rayleigh surface wave but less than the shear wave depending on the interfacial stiffness. If the contacting surfaces are compressed so much that the linear interfacial stiffness is very high, the hysteretic stiffness does not affect the interface wave velocity. However, it has an effect on the speed of interface wave for a loosely contact surfaces with a relatively low linear stiffness. It is also found that the phase velocity of anti-symmetric wave mode converges to the shear wave velocity in despite of the linear stiffness value if the hysteretic stiffness approaches 0.5.

Keywords: Interface Wave, Contact Nonlinearity, Hysteresis, Interfacial Stiffness

1. Introduction

The nonlinearity of contacting surfaces originated from a highly localized plastic deformation of the surface affects the acoustical features in many ways. One way of acoustic measurement of interface stiffness free from the contamination by other source of contact nonlinearity is to use a generalized Rayleigh wave (interface wave) traveling along the contact surface. This wave is a special kind of guided waves occurring in the interface of contacting solids and is affected acoustically by interface stiffness such as the speed of interface wave. The physical nature of contact acoustic nonlinearity(CAN) has been explored by previous researchers including Solodov, Pecorari, and Biwa by developing a linear spring model for contact-type interface(Solodov, 1998; Pecorari and Rokhlin, 2007; and Biwa et al., 2006 and 2007). In their studies, the elasto-plastic behavior of asperities in contact surfaces is considered as a linear spring whose stiffness is linearly proportional to the contact area or the compression load of the interface. This spring model connects the discontinuous displacement of two contacting boundaries with the stresses of the interface by employing the interfacial

Received: November 19, 2010. Revised: December 8, 2010. Accepted: December 10, 2010. *Department of Mechatronic Engineering, Korea University of Technology, 307 Gajun-Ri, Byungchun-Myun, Chunan 330-860, Korea, **Department of Mechanical Engineering, Korea University of Technology and Education, 307 Gajun-Ri, Byungchun-Myun, Chunan 330-860, Korea, †Corresponding Author: nykim@kut.ac.kr

stiffness. However, the hysteresis of the interfacial stiffness is neglected even though experimental reports show that the interfacial stiffness takes different values depending on the loading condition, i.e., either loading or unloading(Kim et al., 2007).

In this paper, the hysteretic characteristic of interfacial stiffness for non-welded contact interface is included in the mathematical spring model to investigate the interface waves along the contact boundaries and to estimate interfacial stiffness by interface wave speed. Dispersion equation of interface waves is derived by combining the wave equation with boundary conditions: discontinuity in both displacement and stress in interface. In the proposed model, a hysteretic interfacial stiffness is introduced to describe the damping behavior of interfacial stiffness. In simulation study, the anti-symmetric mode of interface waves is proved to exist in the hysteretic contact surfaces and be sensitive to the interfacial stiffness in a specific band of acoustic frequency.

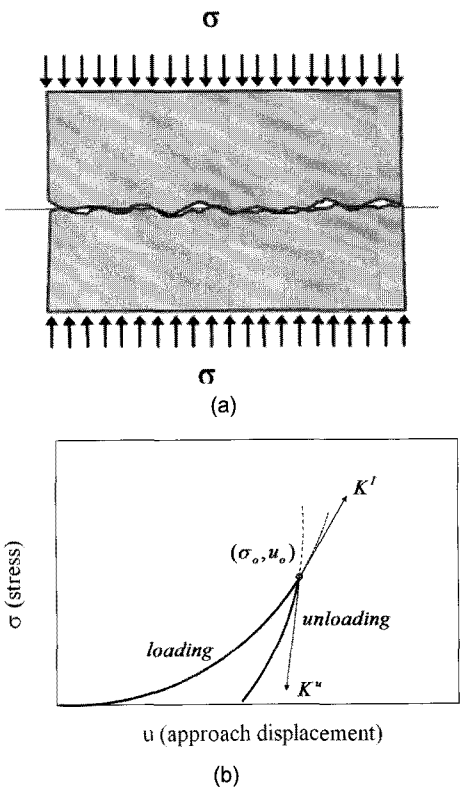

Fig. 1 Hysteresis of interfacial stiffness, (a) Contact surfaces, (b) Stress-approach relation

2. Mathematical Model for Hysteretic Contact Interface

At the micro-scale, contact interface appears as two surfaces of irregular topology which intersect to form micro-void spaces and asperities of contact as shown in Fig. 1(a). The presence of the asperities and voids within planar boundaries makes a thin, compliant zone with effective normal and shear stiffness. The interfacial stiffness can range from near zero for open free surface to almost infinite values for completely welded surfaces which are bonded or subjected to high compressive stresses. Typical stress-displacement (approach) relation of contacting surfaces exhibits a highly nonlinearity as shown in Fig. 1(b) during the loading and unloading. Hysteresis also appears in the stress-displacement curve of Fig. 1(b) during the loading and unloading, indicating the presence of inelastic deformation of the asperities and frictional sliding between contacts. In this case, when a quasi-static load is applied and increased slowly, the approach of the interface boundaries increases along the curve marked as loading in Fig. 1(b). But when the load is released at a certain point(σ_0, u_0), it decreases along a different curve from the loading curve, which is labeled as unloading in Fig. 1(b). Thus the linear stiffness of the interface at (σ_0, u_0) may have a different value according to the loading condition. If it is loading, for instance, the linear stiffness is K^l in Fig. 1(b), but it is K^u when unloading.

This hysteretic behavior can be counted by adopting a spring and damper with complex stiffness connecting two joining surfaces whose stiffness and viscous force vary with the displacement of the contact boundaries. These energy-conservative and energy-dissipative elements are represented in Fig. 2, where the

boundaries are connected by a linear spring and viscous damper in x and z directions. In Fig. 2, the spring and damper are expressed by an equivalent stiffness and damping coefficient in normal and shear directions(z and x) as shown in dotted lines. The spring stiffness K_x and K_z including the damping coefficients are assumed to be independent each other. These hysteretic nonlinear features of contact surfaces are investigated in this paper. Let's reconsider a quasi-equilibrium point (σ_0,u_0) of stress-approach curve in Fig. 1(b). When a disturbance load of acoustic wave is applied, the equilibrium point moves along one of two different paths depending on the nature of loading. If the disturbance is a compression load, it follows the loading curve, but it moves along the unloading curve in Fig. 1(b) when the load is tensile. For each of the loading/unloading curves at the point (σ_0,u_0), the stress variation due to the load can be expressed by the interfacial stiffness and viscosity defined as followings for small deformation in z-direction in Fig. 2,

$$\sigma_z(u)-\sigma_0 = K_z(u_z-u_o)+C_z(\dot{u}_z-\dot{u}_o) \quad (1)$$

In eqn. (1), $\sigma_z(u)$ is the normal stress at the displacement u, K_z and C_z are the linear stiffness and damping coefficient of the interface in the z direction, and the dot sign is the derivative operator in time. Also u_z stands for the displacement(approach) of the interface in the z direction in Fig. 2. Assuming that the damping is a structural damping (Meirovitch, 1967), the damping coefficient C_z may be substituted by an equivalent hysteretic damping coefficient K_{hz} such as $C_z=\frac{K_{hz}}{\omega}$($\omega$: the frequency of acoustic motion). Then the stress-approach relation in eqn. (1) can be expressed by a single complex stiffness $(K_z \pm iK_{hz})$. The reason for the alternative sign in the complex stiffness is that the damping force changes its direction according to the loading condition. While the damping force and spring force are in the same direction in case of loading, they are opposite for unloading. Therefore, the eqn. (1) can be rewritten by the complex stiffness for loading and unloading cases in the z direction, respectively

$$\begin{aligned}\sigma_z(u)-\sigma_0 &= (K_z+iK_{hz})(u_z-u_o) \ \textit{for loading}\\ \sigma_z(u)-\sigma_0 &= (K_z-iK_{hz})(u_z-u_o) \ \textit{for unloading}\end{aligned} \quad (2)$$

In eqn. (2), the complex stiffness $(K_z \pm iK_{hz})$ consists of two components, of which the real part represents a reversible linear elastic behavior of the interface, and the imaginary describes an irreversible hysteretic characteristic of the interface. A similar stress-displacement relation in the x-direction can be obtained in the same manner by using the complex stiffness $(K_z \pm iK_{hz})$. If $K_{hz}=0$ in eqn. (2), the contacting surface acts like purely elastic material, otherwise it has a hysteresis represented by K_{hz}. Now suppose that (u_x^u,u_z^u) and (t_x^u,t_z^u) stand for the displacement and traction of the upper surface in x and z direction, and (u_x^l,u_z^l) and (t_x^l,t_z^l) for the lower surface as shown in Fig. 2. Since both the displacement and stress have discontinuity across the interface, constitutive equations to connect the traction with the displacement on both boundaries are necessary. These conditions are obtained from the stress-displacement relations formulated by eqn. (2) between the tractions and the displacement across the interface in normal and shear directions in Fig. 2.

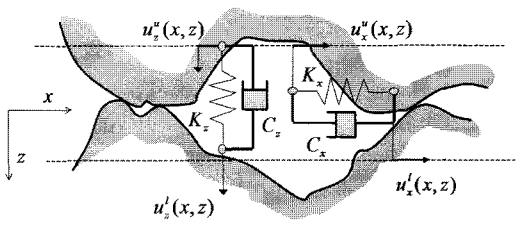

Fig. 2 A spring-damper model for contact surfaces

Assuming that a small deformation takes place at the interface due to external load, two boundaries of the interface move from an initial equilibrium state to a new state independently. Let the initial displacement of the upper and lower surface in z direction be u_z^{uo} and u_z^{lo}, also the new displacement of the upper and lower surface as u_z^u and u_z^l. During this deformation, tractions on both sides are same at the initial state, which is $t_z^{lo} = t_z^{uo} = t_z^o$, but change to t_z^l and t_z^u for the lower and upper surface. At the new position, t_z^l is not necessarily same as t_z^u because of the stress discontinuity of contact interface. In Fig. 2, the deformation of the lower surface made in the positive direction of z imposes an additive compression load to the original traction state t_z^0, while that of the upper surface releases the compression load. Therefore, stress-deformation(approach) relation in the upper surface undergoes a loading process, and the lower surface follows an unloading process. From this consideration, the stress-displacement behavior for both boundaries in x direction can be expressed by using the concept of eqn. (2) as followings,

$$\begin{aligned} t_x^l &= t_x^o + (K_x + iK_{hx})(u_x^l - u_x^u) \\ t_x^u &= t_x^o + (K_x - iK_{hx})(u_x^l - u_x^u) \end{aligned} \tag{3}$$

Or

$$\begin{aligned} \tilde{t}_x^l &= t_x^l - t_x^{lo} = (K_x + iK_{hx})(u_x^l - u_x^u) \\ \tilde{t}_x^u &= t_x^u - t_x^{lo} = (K_x - iK_{hx})(u_x^l - u_x^u) \end{aligned} \tag{4}$$

In eqn. (4), K_x and K_{hx} are the elastic and hysteretic interfacial stiffness of the interface in x direction, and $\tilde{t}_x^l$, $\tilde{t}_x^u$ are the variation of tractions from the original state t_x^o in the lower and upper surface. It can be seen from eqn. (4) that if the hysteretic stiffness K_{hx} is zero, eqn. (4) leads to $t_x^u = t_x^l$, which means that the stress is continuous across the interface. It can also represent the limiting cases for traction-free boundary condition if K_x goes to zero, and for a welded interface as K_x becomes infinity. eqn. (4) gives a complex stiffness model for the nonlinear hysteretic properties of non-welded contact solids. Similar relation for normal stress and displacement in the z direction is obtained in the same way.

3. Formulation of Interface Wave Motions

The dispersion of interface waves along the contact interface have been already proved and demonstrated for the linear elastic model in previous studies (Pecorari and Rokhlin, 2007; Biwa et al., 2006; and Kim et al., 2007). In this section, based on the complex spring model proposed in the previous section, the dispersion equation of interface waves is derived. Interface wave is localized in the interface within a zone that may extend only a few wavelengths away from the boundary, allowing these waves to travel large distance with little reduction in amplitude. The displacement vector for an interface wave propagating along the contact interface in x and z direction with the amplitude that decays exponentially with distance z away from the interface can be expressed for the upper and lower medium as (Kim and Yang, 2007)

$$\begin{aligned} u_x^u(x,z) &= \omega[i\frac{A_1}{c}e^{-p\omega z} + qB_1e^{-q\omega z}]e^{i(\kappa x-\omega t)} \\ u_z^u(x,z) &= \omega[-pA_1e^{-p\omega z} + i\frac{B_1}{c}e^{-q\omega z}]e^{i(\kappa x-\omega t)} \end{aligned} \tag{5}$$

$$\begin{aligned} u_x^l(x,z) &= \omega[i\frac{A_2}{c}e^{+p\omega z} - qB_2e^{+q\omega z}]e^{i(\kappa x-\omega t)} \\ u_z^l(x,z) &= \omega[pA_2e^{+p\omega z} + i\frac{B_2}{c}e^{+q\omega z}]e^{i(\kappa x-\omega t)} \end{aligned} \tag{6}$$

where, ω is the angular frequency, t is time, A_1, A_2, B_1 and B_2 are unknown constants, c is the phase velocity of the interface wave, c_p and c_s are the compression and shear wave velocity respectively, and $p = \sqrt{\frac{1}{c^2} - \frac{1}{c_p^2}}$, $q = \sqrt{\frac{1}{c^2} - \frac{1}{c_s^2}}$. Calculating tractions in the upper and lower

medium by Hooke's law and substituting them into the discontinuity conditions in stress and displacement in eqn. (4) yield four linear equations for four undetermined constants, A_1, A_2, B_1, and B_2. Tractions in the upper and lower medium obtained by substituting eqn. (5) and (6) into Hooke's law are written by

$$\begin{aligned} t_x^u(x,z) &= \omega^2[-2ip\mu\frac{A_1}{c}e^{-p\omega z} - \mu N B_1 e^{-q\omega z}]e^{i(\kappa x-\omega t)} \\ t_z^u(x,z) &= \omega^2[(Lp^2-\frac{\lambda}{c^2})A_1 e^{-p\omega z} - 2i\mu q\frac{B_1}{c}e^{-q\omega z}]e^{i(\kappa x-\omega t)} \\ t_x^l(x,z) &= -\omega^2[2ip\mu\frac{A_2}{c}e^{+p\omega z} - \mu N B_2 e^{+q\omega z}]e^{i(\kappa x-\omega t)} \\ t_z^l(x,z) &= -\omega^2[(Lp^2-\frac{\lambda}{c^2})A_2 e^{+p\omega z} + 2i\mu q\frac{B_2}{c}e^{+q\omega z}]e^{i(\kappa x-\omega t)} \end{aligned} \quad (7)$$

where, λ and μ are Lame's constants, $L=(\lambda+2\mu)$ and $N=(c^{-2}+q^2)$. Substituting eqn. (5), (6) and (7) into the nonlinear displacement discontinuity condition given by eqn. (4) yields a system of four homogeneous linear equations for four undetermined constants, A_1, A_2, B_1 and B_2, which is given by

$$\begin{bmatrix} \frac{i}{c}(2K_x+2\mu\omega p) & (2qK_x+\mu\omega N) & -\frac{i}{c}(2K_x+2\mu\omega p) & (2qK_x+\mu\omega N) \\ (2pK_z-\omega Q) & -\frac{i}{c}(2K_z+2\mu\omega q) & (2pK_z-\omega Q) & \frac{i}{c}(2K_z+2\mu\omega q) \\ \frac{1}{c}(2i\mu\omega p-2K_{hx}) & (2iqK_{hx}+\mu\omega N) & \frac{1}{c}(2i\mu\omega p+2K_{hx}) & (2iqK_{hx}-\mu\omega N) \\ (2ipK_{hz}-\omega Q) & -\frac{1}{c}(2i\mu\omega q-2K_{hz}) & (2ipK_{hz}+\omega Q) & -\frac{1}{c}(2i\mu\omega q+2K_{hz}) \end{bmatrix} \begin{Bmatrix} A_1 \\ B_1 \\ A_2 \\ B_2 \end{Bmatrix} = \{0\} \quad (8)$$

where, $Q=(\lambda c^{-2}-Lp^2)$. Examining the first two equations of eqn. (8) reveals that only two combinations of solutions are possible corresponding to:

i) $A_2 = -A_1$, $B_2 = B_1$ (9)

ii) $A_2 = A_1$, $B_2 = -B_1$ (10)

Replacing A_2 and B_2 with A_1 and B_1 in eqn. (8) by using eqn. (9) and (10) produces two wave motions, one is symmetric about the interface, and the other is anti-symmetric about the interface. For the conditions $A_2=-A_1$, $B_2=B_1$ provoking the anti-symmetric motion, eqn. (8) reduces to

$$\begin{bmatrix} \frac{2i}{c}(K_x+\mu\omega p) & 2qK_x+\mu\omega N \\ -\frac{2}{c}K_{hx}-\omega Q & 2iq(K_{hx}-\frac{\mu\omega}{c}) \end{bmatrix} \begin{Bmatrix} A_1 \\ B_1 \end{Bmatrix} = \{0\} \quad (11)$$

In order for eqn. (11) to have a non-trivial solution, the determinant of the coefficient matrix of eqn. (11) must be zero, which is,

$$c_s^4[\frac{4pq}{c^2}+N\frac{Q}{\mu}]+\frac{K_x}{\mu\omega}\cdot 2qc_s^2+\frac{K_{hx}}{\mu\omega}\frac{2c_s^4}{c}[N-2pq]=0 \quad (12)$$

Substituting the definitions of N, Q, p, and q into eqn. (12) and rewriting it with dimensionless quantities gives the dispersion equation for anti-symmetric motion in nonlinear contact interface in more concise expression

$$\begin{aligned} &[4\alpha^2\sqrt{\alpha^2-1}\cdot\sqrt{\alpha^2-\beta^2}-(1-2\alpha^2)^2]+2(\frac{K_x}{\omega Z_s})\sqrt{\alpha^2-1} \\ &\quad +2(\frac{K_{hx}}{\omega Z_s})\alpha[2\alpha^2-2\sqrt{\alpha^2-1}\cdot\sqrt{\alpha^2-\beta^2}-1]=0 \end{aligned} \quad (13)$$

where, $\alpha=\frac{c_s}{c}$, $\beta=\frac{c_s}{c_p}$, $Z_s=\rho c_s$ is the shear acoustic impedance of the medium and $\frac{K_x}{\omega Z_s}$, $\frac{K_{hx}}{\omega Z_s}$ are the linear and hysteretic specific shear stiffness in the x direction. In the same manner, the dispersion equation for the symmetric wave motion of nonlinear contact interface is obtained by substituting eqn. (10) into eqn. (8). For the symmetric motion, $A_2=A_1$, $B_2=-B_1$, eqn. (8) is written by

$$\begin{bmatrix} (2pK_z-\omega Q) & -\frac{i}{c}(2K_z+2\mu\omega q) \\ 2i(pK_{hz}+\frac{1}{c}\mu\omega p) & \frac{2}{c}K_{hz}+\mu\omega N \end{bmatrix} \begin{Bmatrix} A_1 \\ B_1 \end{Bmatrix} = \{0\} \quad (14)$$

eqn. (14) leads to the following necessary condition for a non-trivial solution,

$$\mu\omega[QN+\frac{4}{c^2}\mu pq]+K_z\cdot 2p\mu+K_{hz}\cdot\frac{2\mu}{c}[2pq+\frac{Q}{\mu}]=0 \quad (15)$$

Putting the definitions of N, Q, p, and q into eqn. (15) and rewriting it with dimensionless

quantities, α and β, gives the dispersion equation for symmetric motion in contact interface in compact form as follows

$$[4\alpha^2\sqrt{\alpha^2-1}\cdot\sqrt{\alpha^2-\beta^2}-(1-2\alpha^2)^2]+2(\frac{K_z}{\omega Z_s})\sqrt{\alpha^2-\beta^2} + 2(\frac{K_{hz}}{\omega Z_s})\alpha[2\alpha^2-2\sqrt{\alpha^2-1}\cdot\sqrt{\alpha^2-\beta^2}-1]=0 \quad (16)$$

where, $\frac{K_Z}{\omega Z_s}$, $\frac{K_{hz}}{\omega Z_s}$ are the linear and hysteretic specific normal stiffnesses. Eqn. (13) and (16) are the complete dispersion equations describing the interface waves propagating along the hysteretic contact interface. It is clear that the first terms of eqn. (13) and (16) represent the free Rayleigh equation for the free boundary condition. If the interface is free of stress, i.e., $K_x = K_{hx} = K_Z = K_{hz} = 0$, the dispersion equation of eqn. (13) and (16) becomes the famous Rayleigh characteristic equation, which is given by,

$$4\alpha^2\sqrt{\alpha^2-1}\cdot\sqrt{\alpha^2-\beta^2}-(1-2\alpha^2)^2=0 \quad (17)$$

In terms of the velocities of shear, normal, and interface waves, the above equation is expressed as

$$4\sqrt{1-\frac{c^2}{c_s^2}}\cdot\sqrt{1-\frac{c^2}{c_l^2}}-(2-\frac{c^2}{c_s^2})^2=0 \quad (18)$$

Second and third term of eqn. (13) and (16) result from the linear and hysteretic contact of interface surfaces, respectively. The angular frequency ω included in eqn. (13) and (16) indicates that the interface waves are dispersive, so that the wave velocity varies with the frequency as well as material properties such as contact stiffness. The symmetric and anti-symmetric waves represented by eqn. (13) and (16) are a guided waves, which can be schematized in Fig. 3. They degenerate to the Rayleigh waves on the free surface when the dimensionless linear and hysteretic interface stiffnesses are zero. If they are finite, unlike the Rayleigh equation, eqn. (13) and (16) become

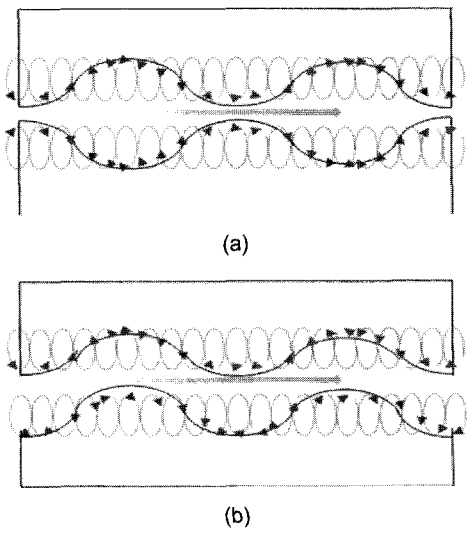

Fig. 3 Symmetric (a) and Anti-symmetric (b) Mode of interface waves

dispersive. eqn. (13) and (16) also show that the symmetric wave mode comes from the normal coupling between the surfaces of the interface and the anti-symmetric wave from the tangential shear coupling.

In order for the interface waves to exist and propagate, eqn. (13) and (16) should have real roots. However, the symmetric wave motion of eqn. (16) doesn't have real roots at all regardless of the magnitude of the linear and nonlinear stiffness. Therefore the symmetric wave does not exist all the time. From eqn. (13) it is obvious that the ant-symmetric wave has real roots even though the hysteretic stiffness K_{hx} is present. Moreover, the anti-symmetric mode is always found in the interface because K_{hx} is small comparing to K_x in reality.

4. Dispersion of Anti-Symmetric Waves

Fig. 4 describes the dispersion curves of the interface wave (anti-symmetric mode) as a function of frequency when the hysteretic stiffness is negligible. In Fig. 4, the phase speed of the interface wave in the contact surface of three different stiffness values from 10 GPa/m to

1000 GPa/m is displayed. As the frequency of the interface wave increases, the interface wave velocity increases together. However for a low frequency wave less than 0.01 MHz, the interface wave speed is almost same as the shear wave velocity and does not change much with the frequency no matter how large the interfacial stiffness is. Also in the high frequency range above 10 MHz, it becomes close the speed of Rayleigh surface wave and change little with the linear stiffness K_x. But it increases remarkably between 0.01 MHz and 10 MHz even though the sensitive band depend on the stiffness and material property(acoustic impedance). It asymptotes to the shear wave velocity as the frequency increases up to few MHz order. In Fig. 5, the phase velocity ratio, $\alpha = \frac{c_s}{c}$, is plotted against the linear interfacial stiffness K_x to investigate the effect of the linear stiffness on the dispersion of interface waves. It changes very little in the range of low specific stiffness below than 0.01, but increases very rapidly between 0.01 and 10, and finally saturates above 10. In an interface of low linear stiffness, the interface wave propagates with the speed of Rayleigh surface wave no matter what material the interface is made of. But it moves faster and up to the speed of shear wave, c_s, when the stiffness K_x increases. The smaller the velocity ratio $\beta = \frac{c_s}{c_p}$ is, the slower the interface wave becomes. Thus Fig. 5 implies that the interface wave velocity can indicate a contacting state of the interface. When the interface is closed and compressed very tight, so that the linear stiffness gets large, the interface wave speed becomes faster than the Rayleigh surface wave. On the contrary it approaches the Rayleigh wave if the interface is open and free.

Finally, the effect of hysteretic stiffness K_{hx} on the dispersion is illustrated in Fig. 6. Unlike the linear stiffness, the speed of interface wave monotonically decreases with the increase of

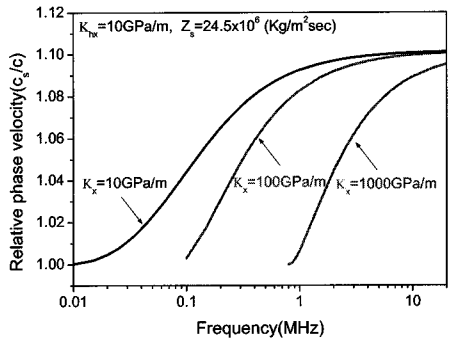

Fig. 4 Dispersion of anti-symmetric mode wave when $K_{hx} = 0$

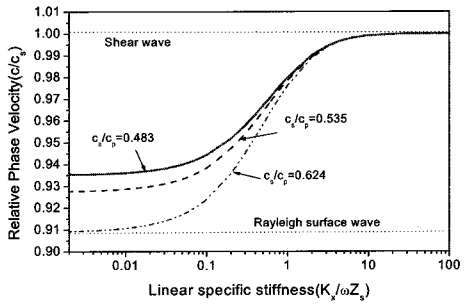

Fig. 5 Dispersion curves of anti-symmetric mode wave for different materials

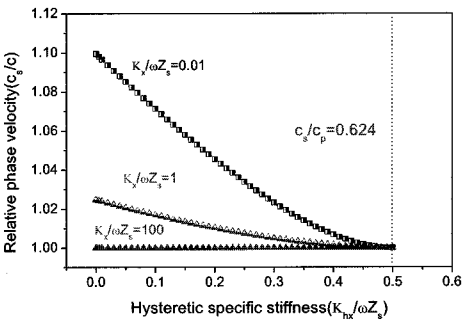

Fig. 6 Phase velocity of anti-symmetric mode wave with respective to $\frac{K_{hx}}{\omega Z_s}$

specific hysteretic stiffness $\frac{K_{hx}}{\omega Z_s}$ for all linear stiffness values. It approaches an asymptotic value, the shear wave velocity, when $\frac{K_{hx}}{\omega Z_s}$ goes near 0.5, no matter how high the linear stiffness is. If the specific hysteretic stiffness $\frac{K_{hx}}{\omega Z_s}$

becomes higher than the critical value, no interface wave can propagate or exist. Interesting fact is that the hysteretic stiffness does affect very much the interface wave speed for an interface with low linear stiffness, while it does not for the high linear stiffness. This means that the hysteresis of an interface plays an important role on the dispersive characteristic when the interface is weakly closed. But it has no effect on the dispersion of the interface waves if the interface is closed very tight under compression like an early fracture surfaces. In Fig. 6, the interface speed is not affected by the hysteretic stiffness for an interface of high linear specific stiffness more than about 100. However, for the interface with linear stiffness less than $\frac{K_x}{\omega Z_s}=0.1$, the phase velocity decreases significantly with the increase of the hysteretic stiffness. In the limiting case that the hysteretic stiffness $\frac{K_{hx}}{\omega Z_s}$ approaches 0.5 in Fig. 6, the phase velocity of interface wave asymptotes to the Rayleigh wave velocity regardless of the linear stiffness and material properties. No propagating waves exist beyond the value of $\frac{K_{hx}}{\omega Z_s}=0.5$ as shown in Fig. 6, where the phase velocity of the anti-symmetric interface wave is bounded to the shear wave velocity regardless of K_x.

It is also found from Fig. 6 that the linear stiffness K_x plays a key role too in the dispersion characteristics in entire region. Phase velocity is increased up to 10% by the increase of the linear stiffness K_x. On the contrary to the hysteretic stiffness, the higher linear stiffness makes the interface wave faster. However, if the linear stiffness K_x is high enough as represented in Fig. 6, the phase velocity is almost constant and insensitive to the hysteretic stiffness K_{hx}. It can be deduced that this dependency of interface wave velocity on the linear and hysteretic stiffnesses can be used to analyze and estimate the contact state of non-welded interface such as partly closed cracks.

5. Conclusions

Interface waves of contact interface with hysteresis are demonstrated in theory to exist based on a spring model that has a complex stiffness. Hysteretic linear model for contact interface is developed to relate discontinuous displacements with tractions on both sides of the contact interface by employing the hysteretic interfacial stiffness. Analytic formulation of the interface waves and solutions to the wave equations are derived to obtain the dispersion equations for the symmetric and anti-symmetric interface waves. Analysis of the dispersion equations shows that the symmetric mode does not exist and only anti-symmetric mode can propagate along the interface as a guided wave if the hysteretic specific stiffness is small less than 0.5. Theoretical results verify that the phase velocity and hysteresis of the anti-symmetric wave is sensitive to contact state and the wave speed changes as much as 10% depending on both the linear and hysteretic stiffness. It is also proved that the phase velocity of the anti-symmetric wave is bounded between the shear wave velocity and the Rayleigh wave velocity even when the hysteretic stiffness is included. It can be concluded that interface waves can be used effectively to estimate the contact stiffness or fracture state.

Acknowledgments

Authors gratefully acknowledge the support to this work by the Ministry of Education, Science and Technology in Korea (MEST).

References

Biwa, S., Hiraiwa, S. and Matsumoto, E. (2006) Experimental and Theoretical Study of Harmonic

Generation at Contacting Interface, *Ultrasonics,* Vol. 44, pp. 1319-1322

Biwa, S., Hiraiwa, S. and Matsumoto, E. (2007) Stiffness Evaluation of Contacting Surfaces by Bulk and Interface Waves, *Ultrasonics,* Vol. 47, pp. 123-129

Kim, J. Y., Baltazar, A. and Rokhlin, S. I. (2004), Ultrasonic Assessment of Rough Surface Contact between Solids from Elasto-Plastic Loading-Unloading Hysteresis Cycle, *Journal of the Mechanics and Physics of Solids*, Vol. 52, pp. 1911-1934

Kim, N and Yang, S (2007) Nonlinear Displacement Discontinuity Model for Generalized Rayleigh Wave in Contact Interface, *Journal of the Korean Society for Nondestructive Testing,* Vol. 27, No. 6, pp. 582-590

Meirovitch, L. (1967) *Analytical Methods in Vibrations,* MaCmillan Company, New York, USA, pp. 403-404

Pecorari, C. and Rokhlin, S. I. (2007) Elasto-Plastic Micromechanical Model for Determination of Dynamic Stiffness and Real Contact Area from Ultrasonic Measurements, *Wear*, Vol. 262, pp. 905-913.

Solodov, I. Y. (1998) Ultrasonics of Non-Linear Contacts: Propagation, Reflection, and NDE Applications, *Ultrasonics,* Vol. 36, pp. 383-390